Tailoring Upper-Limb Robot-Aided Orthopedic Rehabilitation on Patients' Psychophysiological State

Christian Tamantini, *Member, IEEE*, Francesca Cordella, *Member, IEEE*, Clemente Lauretti, *Member, IEEE*, Francesco Scotto di Luzio, *Member, IEEE*, Benedetta Campagnola, Laura Cricenti, Marco Bravi, Federica Bressi, Francesco Draicchio, Silvia Sterzi, and Loredana Zollo, *Senior Member, IEEE*

***Abstract*— Physical therapy keeps exploiting more and more the capabilities of the robot of adapting the treatments to patients' needs. This paper aims at presenting a psychophysiological-aware control strategy for upper limb robot-aided orthopedic rehabilitation. The main features are the capability of i) generating point-to-point trajectories inside an adaptable workspace, ii) providing assistance in guiding the patients' limbs in accomplishing the assigned task allowing them to freely move with a certain degree of spatial and temporal autonomy and iii) tuning the control parameters according to the patients' kinematics performance and psychophysiological state. The implemented control strategy is validated in a real clinical setting on eight orthopedic patients undergoing twenty daily robot-aided rehabilitation sessions. The psychophysiological-aware control strategy evidenced a positive impact on the enrolled participants since they are effectively conducted in a calmer condition with respect to the patients who did not receive the psychophysiological adaptation. Moreover, clinical performance indicators suggest that the proposed tailored control strategy improves motor functions.**

Manuscript received 15 February 2023; revised 14 June 2023; accepted 13 July 2023. Date of publication 24 July 2023; date of current version 18 August 2023. This work was supported in part by Regione Lazio with Healthcare Agents and Learning Robots (HeAL9000) Project CUP: B84I20001880002, in part by the Italian Institute for Labour Accidents (INAIL) with Portable Exoskeleton for Rehabilitation and Assistance of a Patient Suffering from Plexus Injury (BioARM) under Grant CUP: E58D19000650005, and in part by the SPINE 4.0 Project CUP: C85F21001020001. *(Christian Tamantini and Francesca Cordella contributed equally to this work.) (Corresponding author: Christian Tamantini.)*

This work involved human subjects or animals in its research. Approval of all ethical and experimental procedures and protocols was granted by the Ethical Committee under Approval No. 03/19 PAR ComEt CBM, and performed in line with the Declaration of Helsinki.

Christian Tamantini, Francesca Cordella, Clemente Lauretti, Francesco Scotto di Luzio, and Loredana Zollo are with the Research Unit of Advanced Robotics and Human-Centered Technologies, Universitá Campus Bio-Medico di Roma, 00128 Rome, Italy (e-mail: c.tamantini@unicampus.it).

Benedetta Campagnola, Laura Cricenti, Federica Bressi, and Silvia Sterzi are with the Unit of Physical Medicine and Rehabilitation, Universitá Campus Bio-Medico di Roma, 00128 Rome, Italy.

Marco Bravi is with the Unit of Physical Medicine and Rehabilitation, Universita Campus Bio-Medico di Roma, 00128 Rome, Italy, and also with the Department of Movement, Human and Health Sciences, University of Rome "Foro Italico", 00135 Rome, Italy.

Francesco Draicchio is with the Department of Occupational and Environmental Medicine, INAIL, Monte Porzio Catone, 00078 Rome, Italy.

Digital Object Identifier 10.1109/TNSRE.2023.3298381

***Index Terms*— Rehabilitation robotics, human-centered robotics, human–robot interaction, psychophysiological state estimation.**

I. Introduction

MUSCULOSKELETAL Disorders (MSDs) are one of the leading causes of severe long-term pain and physical disability [1]. The people who are most affected by musculoskeletal disorders are workers exposed to biomechanical overload of the upper limbs and the elderly who suffer from sarcopenia, tendinopathies, and arthritis [2], [3], [4]

Robot-aided rehabilitation might play an essential role in treating MSDs to allow patients to recover their motor performance. However, the adoption of robot-aided orthopedic rehabilitation is limited to very few studies [5], [6]. Patients affected by MSDs are expected to restore their motor functional Ranges of Motion (RoM), improve their muscular strength, and reduce pain [7], [8]. More in general, a robotic platform for robot-assisted orthopedic rehabilitation should be able to guide the patients' limbs in performing tasks with a customized level of assistance and modify trajectories according to the patients' RoM recovery. Furthermore, in rehabilitation treatments for orthopedic patients, the affected limbs or joints should not be overloaded by repetitive movements, as is the case in neurorehabilitation, to avoid fatigue and/or the occurrence of pain.

Robot control law should allow the patients to freely move in space and in time (spatial and temporal autonomy, namely) to accomplish the proposed tasks. Furthermore, the controller parameters should be adapted according to the patients' kinematics performance, to provide more and more specific robot interventions, and to their psychophysiological state, to maximize their active involvement in the rehabilitation and enhance their experience in interacting with the rehabilitation robot [9]. Several control strategies have been proposed to exert the minimum assistance to increase patients' spatial autonomy [10]. Force or velocity fields can be defined in the rehabilitation workspace to provide assistance according to the patients' limb position. A fault-tolerant region along with a constantly sliding wall is introduced in [11]. The resulting assistance moves the patients forward along the desired path with a constant speed without allowing the patients, enrolled to

validate the system (an elderly female), to decide self-peaced motion velocity.

In order to increase patients' temporal autonomy, velocity field approaches have been designed in the literature. The reference velocity profile is computed according to patients' limb position instead of defining a time law [12]. On the other hand, velocity field controllers do not allow the user to move arbitrarily fast along the desired path and the assistance level provided cannot be adjusted according to patients' motor performance.

As outlined in the literature, tailoring the robotic treatment with patients parameters (kinematic, muscular and force) improves motor recovery [13], [14], [15].

Indeed, the so-called biocooperative systems aim at closing the control loop on patients [16]. Kinematics performance can be directly used to tune the control parameters according to the user needs [17]. Similarly, patients physiological parameters can serve as input to adapt the robot control in gait [18], [19] as well as in upper limb robot-aided rehabilitation [20].

Apart from the raw physiological measurement, the psychophysiological state of the patients may play an essential role in adapting the robot's behavior to improve the patients' experience during the interaction with the robot [21]. Most of the literature research models the psychophysiological state according to Russell representation [22]. Each state can be represented by two dimensions: Arousal and Valence. The former indicates the user's involvement in executing a certain activity or in general after the administration of a stimulus. The latter defines whether the elicited state assumes a positive or negative meaning. Some studies demonstrated that the human-robot interaction influences the users' psychophysiological state [23]. Similarly, the estimation of the patients' state can be used to trigger audiovisual stimuli of the rehabilitation platform provided by means of virtual reality environments [24], [25], [26]. Anyhow, robot-aided rehabilitation platforms can be exploited to provide many different kinds of feedback and modulate human-robot interaction.

Nevertheless, a comparative analysis between patient-tailored rehabilitation and conventional robot-aided rehabilitation has not been performed. In particular, no study has investigated the possibility of improving human-robot interaction during robot-assisted rehabilitation sessions by exploiting the estimation of the patients' psychophysiological state. Indeed, we want to demonstrate that adapting the control parameters in a patient-tailored manner has an effect on the patients' robot perception and on its motor recovery.

For this reason, the objective of this paper is to propose and validate a psychophysiological-aware control strategy for robot-aided orthopedic rehabilitation to tailor the treatment according to patients' motor performance and psychophysiological state. It is worth investigating whether a more personalized approach is capable of increasing the robot's adaptability to a specific patient as well as patients' active participation in treatment while also optimizing the clinical outcomes. To this purpose, the proposed approach is implemented onto an end-effector robot in a clinical protocol composed of twenty sessions and delivered to eight patients suffering from outcomes of orthopedic surgery. The effectiveness of the proposed controller is quantified in terms of psychophysiological modifications induced during the patient-robot interaction and motor recovery over time.

The paper is structured as follows: Section II details the proposed robotic architecture and its experimental validation in the clinical scenario. Section III outlines and discusses the emerging results and Section IV draws the conclusion and delineates future work.

II. Materials and Methods

An overview of the proposed robotic architecture is presented in Fig. 1. As evidenced, to implement the psychophysiological-aware control strategy, the trajectory planner module generates a path P in Cartesian space and a current desired position $\mathbf{p_W}(t)$, called desired back-wall position in the following. The Assist-as-needed (AAN) controller implements an inverse dynamic control law to infer the robot joints control torques τ_c from the computation of the total assistive acceleration by summing two terms, namely the tunnel and back-wall contributions. The former aims at maintaining the robot's end-effector, and therefore the patients' limb, within a space region defined as a tunnel. The latter provides assistance to the patients to direct them toward task completion. In particular, a back-wall advances from the initial position $\mathbf{p_i}$ and pushes the patients forward. The main core of the proposed approach lies in tailoring the interaction to the kinematic performance and psychophysiological state of the patients. In fact, the stiffness of the robotic system is adapted according to kinematic measurements, collected in specific evaluation sessions, and daily based on the patients' state estimated from multimodal physiological monitoring. In the following, all the functional blocks are explained in detail.

A. Trajectory Planner

The trajectory planner computes the path that the patients have to follow P and the desired back-wall position $\mathbf{p_W}(t)$, per each time instant t. It takes as input the initial position $\mathbf{p_i}$, the final target position $\mathbf{p_f}$, the pause time T_P, i.e. a time to let the patients autonomously initiate the exercise without generating any robot intervention, and the time to accomplish the task T_F. To enable patients to independently initiate the movement, the position of the back wall, denoted as $\mathbf{p_W}(t)$, remains constant at $\mathbf{p_i}$ for a duration of T_P seconds. Otherwise, if the patient is taking more than T_P seconds to start moving, the back-wall moves forward the user limb in accomplishing the assigned task in T_F seconds. In this way, the trajectory planner generates a time law describing the position of an advancing wall $\mathbf{p_W}(t)$, orthogonal to the desired path, used by the controller to provide assistance to move the patient's limb toward the target only if he/she takes more than the defined time to complete the task. The path that the patients have to follow with the assistance of the robot in the specific motor task can vary, ranging from simple point-to-point straight movements up to complex trajectories that replicate activities of daily life, such as work-related gestures [27]. In the treatment of orthopedic patients, robotic rehabilitation allows patients to be trained to gradually reach farther

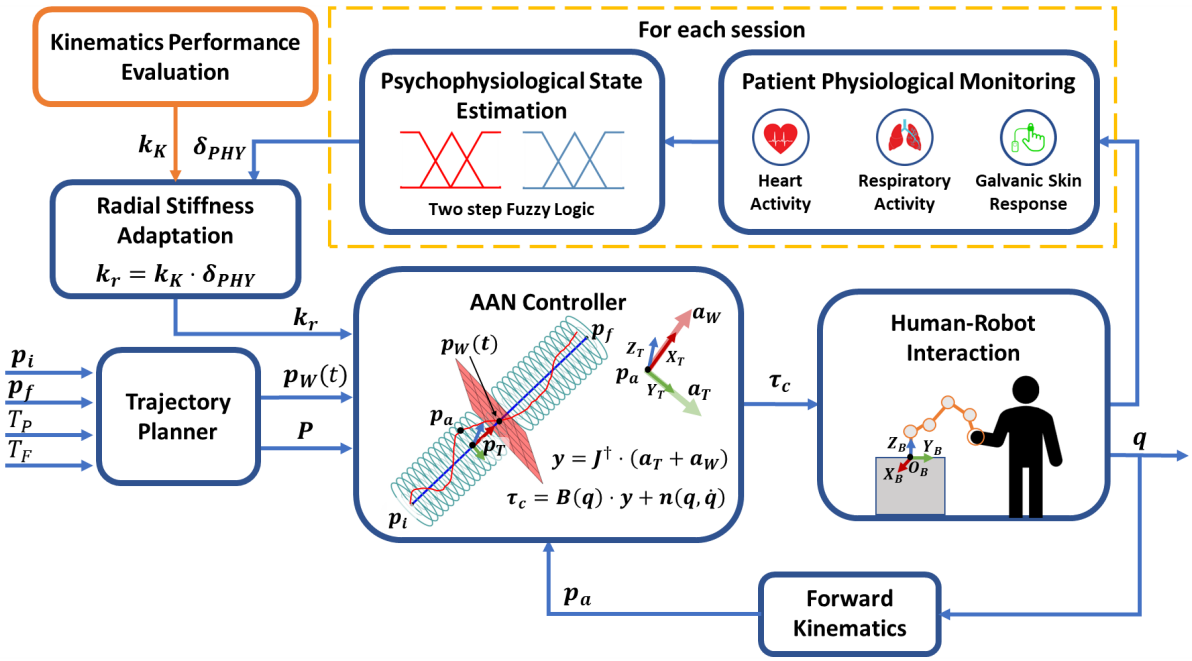

Fig. 1. Block scheme of the presented psychophysiological-aware Control architecture for orthopedic robot-aided rehabilitation.

points in three-dimensional space. Consequently, the trajectory planner implemented in this work returns straight segments in Cartesian space managing different initial and final positions, $\mathbf{p_i}$ and $\mathbf{p_f}$, respectively. A graphical representation of the back-wall position, planned by the trajectory planner, is depicted in Fig. 2B.

B. Patient-Tailored Control

The proposed approach is grounded on an inverse dynamics control law. Its stiffness parameters are tuned according to the patients kinematics and psychophysiological state. The control law is defined as

$$\tau_c = \mathbf{B}(\mathbf{q})\mathbf{y} + \mathbf{C}(\mathbf{q}, \dot{\mathbf{q}})\dot{\mathbf{q}} + \mathbf{F}_v\dot{\mathbf{q}} + \mathbf{F}_s sign(\dot{\mathbf{q}}) + \mathbf{g}(\mathbf{q}) \quad (1)$$

where $\mathbf{B}(\mathbf{q})$ is the robot inertia matrix, $\mathbf{C}(\mathbf{q}, \dot{\mathbf{q}})$ accounts for centrifugal and Coriolis effects, $\mathbf{F}_v$ is the viscous friction torque, $\mathbf{F}_s sign(\dot{\mathbf{q}})$ is the static friction torque, $\mathbf{g}(\mathbf{q})$ is the gravity contribution, $\mathbf{q}$, $\dot{\mathbf{q}}$ and $\ddot{\mathbf{q}}$ are the robot joint position, velocity and acceleration, respectively, τ_c is the joint torques and $\mathbf{y}$ represents joint space accelerations containing the stabilising actions [28]. In particular, $\mathbf{y}$ is modelled as

$$\begin{cases} \mathbf{y} = \mathbf{J}^{\dagger}(\mathbf{q})(\mathbf{a}_T + \mathbf{a}_W) \\ \mathbf{a}_T = \mathbf{Ad}_t^{-1}\mathbf{K}_T\mathbf{Ad}_t\tilde{\mathbf{x}}_T \\ \mathbf{a}_W = \mathbf{Ad}_t^{-1}\mathbf{K}_W\mathbf{Ad}_t\tilde{\mathbf{x}}_W \end{cases} \quad (2)$$

where $\mathbf{J}^{\dagger} = \mathbf{J}^T\left(\mathbf{J}\cdot\mathbf{J}^T\right)^{-1}$ is the right pseudo-inverse matrix of the robot geometric Jacobian, $\tilde{\mathbf{x}}_T = [\tilde{\mathbf{p}}_T; \tilde{\varphi}_T]$ and $\tilde{\mathbf{x}}_W = [\tilde{\mathbf{p}}_W; \tilde{\varphi}_W]$ are the pose errors of the actual end-effector pose $\mathbf{x}_a = [\mathbf{p}_a, \varphi_a]$ with respect to the tunnel and back-wall pose, respectively, expressed in the robot base fixed reference frame $[\mathbf{X}_B, \mathbf{Y}_B, \mathbf{Z}_B]$. In particular, the tunnel pose $\mathbf{x}_T$ is the nearest on the planned path P with respect to the end-effector actual one. The back-wall pose $\mathbf{x}_W$ coincides with the output of the trajectory planner (see Section II-A). It is worth observing that Eq. (2) does not take into account the desired end-effector velocity and acceleration ($\dot{\mathbf{x}}_d$ and $\ddot{\mathbf{x}}_d$) since the controller aims at generating a force field without an explicit time law.

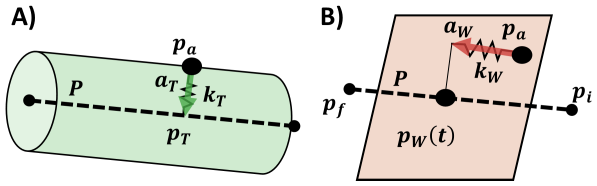

Fig. 2. Control contributions generated by the proposed controller, i.e. A) tunnel and B) back wall.

The pose errors $\tilde{\mathbf{x}}_T$ and $\tilde{\mathbf{x}}_W$, expressed in the base reference frame, are transformed into a moving frame $[\mathbf{X}_T, \mathbf{Y}_T, \mathbf{Z}_T]$ by means of the adjoint matrix (see Eq. (2)). The vector tangential to the planned path P, centered in $\mathbf{p}_T$, is used to compute the $\mathbf{X}_T$ axis of the moving frame. $\mathbf{Y}_T$ and $\mathbf{Z}_T$ axes are chosen arbitrarily to be orthogonal to $\mathbf{X}_T$. Ultimately, $\mathbf{Ad}_t$ is expressed as

$$\mathbf{Ad}_t = \begin{bmatrix} \mathbf{R}_T^B & \hat{\mathbf{p}}_T\mathbf{R}_T^B \\ \mathbf{O}_{(3\times3)} & \mathbf{R}_T^B \end{bmatrix}^T \quad (3)$$

where $\mathbf{R}_T^B$ is the rotation matrix that expresses the orientation of the moving frame $[\mathbf{X}_T, \mathbf{Y}_T, \mathbf{Z}_T]$ with respect to the base frame and $\hat{\mathbf{p}}_T$ is the skew-symmetric matrix of the tunnel position $\mathbf{p}_T$. The controller generates two assistive contributions: the tunnel and the back wall. A graphical representation of the control contributions generated by the controller is provided in Fig. 2. The $\mathbf{a}_T$ control action, reported in 2A, maintains the robot end-effector near the planned path P. The back-wall contribution $\mathbf{a}_W$, shown in Fig. 2B, moves forward the patients in accomplishing the assigned trajectory

in T_F seconds. The stiffness matrices $\mathbf{K_T}$ and $\mathbf{K_W}$ encode the robot behavior in generating the tunnel and back-wall assistive contributions, respectively. Both matrices are (6×6) positive-defined diagonal as $\mathbf{K}_T = diag\{0, k_r, k_r, k_\phi, k_\phi, k_\phi\}$ and $\mathbf{K}_W = diag\{\hat{k}_w, 0, 0, 0, 0, 0\}$ where k_r manages the radial stiffness around the tunnel, k_ϕ is the orientation control gain and $\hat{k}_w$ is the back-wall stiffness along the X_T axis. In particular, $\hat{k}_w$ assumes different values as

$$\hat{k}_w = \begin{cases} k_w, & \langle \tilde{\mathbf{p}_W}, \mathbf{X_T} \rangle \geq 0 \\ 0, & \langle \tilde{\mathbf{p}_W}, \mathbf{X_T} \rangle < 0 \end{cases} \tag{4}$$

where the $\langle \cdot, \cdot \rangle$ operator represents the dot products between two vectors, which means that the $\mathbf{a}_W$ accelerations are supplied whenever the current end-effector position is behind the back-wall one.

The robotic architecture proposed in this paper takes into account the kinematic performance of the patients as well as their psychophysiological state. In particular, the radial stiffness k_r implemented onto the rehabilitation robot is computed as

$$k_r = k_K \cdot \delta_{PHY} \tag{5}$$

where k_K is the stiffness retrieved from the kinematics assessment and δ_{PHY} represents the daily adaptation of the robot stiffness according to the psychophysiological state of the patients (see Section II-C.2). The motor performance mostly drives the definition of the current robot stiffness while the psychophysiological component acts as a multiplicative factor to adjust the radial stiffness. It is worth observing that the back wall impacts mainly on the task speed, requiring the patients a physical workload. On the other hand, radial stiffness affects task accuracy, involving significant cognitive workload. The user's psycho-physiological state slightly varies with task speed and physical load, but it is significantly impacted by the patients' cognitive load.

C. Radial Stiffness Modulation

1) Modulation Based on Kinematic Performance: In order to tune the level of assistance tailored to patients' specific needs, the robot stiffness is modulated on the basis of patients performance [17]. More in detail, the motor performance of the patients is evaluated during the execution of point-to-point movements without the robot's assistance by using the normalized angle between the assigned direction $\overrightarrow{v_d}$ and the effective task directly from the starting point up to the point of peak speed $\overrightarrow{v_p}$. The aiming angle α quantifies the patients' capability to perform a motion along the desired direction. The higher the α, the lower the patients performance. It is computed as

$$\alpha = \frac{1}{\pi} \left| \arccos \left(\frac{\langle \overrightarrow{v_d}, \overrightarrow{v_p} \rangle}{\| \overrightarrow{v_d} \| \| \overrightarrow{v_p} \|} \right) \right|. \tag{6}$$

A preliminary analysis showed that subjects obtaining an aiming angle value < 0.3 were able to track the desired trajectory requiring minimum robot intervention. On the contrary, a higher α (≥ 0.3) needed more significant corrective actions to ensure trajectory tracking. In particular, for

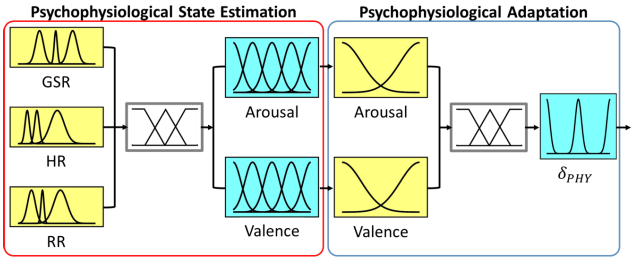

Fig. 3. Schematic representation of the two-step Fuzzy Logic Model implemented to estimate the psychophysiological adaptation starting from physiological parameters.

$\alpha < 0.1$, $0.1 \leq \alpha < 0.3$ and $0.3 \leq \alpha < 1$, k_K assumes the discrete values $\{0.1, 300, 1000\}$ N/m, respectively. The choice of specific robot stiffness levels is crucial and is based on standardization. It is important for the sake of comparability and reproducibility. A predefined set of stiffness levels allows easier comparisons of the results to evaluate the effectiveness of the rehabilitation treatment across diverse pathological populations [10], [29].

2) Modulation Based on Psycophysiological State Estimation: The patients psychophysiological state estimation for the stiffness adaptation is implemented by means of a two-layer Fuzzy Logic inference system, reported in Fig. 3. The first one aims at estimating the psychophysiological state in terms of Arousal (**A**) and Valence (**V**) by exploiting a wearable physiological monitoring system. The second layer takes as input the estimated psychophysiological state and computes the psychophysiological adaptation factor δ_{PHY}. The patients physiological monitoring system measures the Heart Rate (HR), the Respiratory Rate (RR) activities, and the Galvanic Skin Response (GSR). Starting from the acquired GSR signal, the tonic component, also called Skin Conductance Level, is computed by applying a 4^{th} order Butterworth low-pass filter, with a cutoff frequency of 0.1 Hz.

Given the high intra- and inter-subject variability of physiological signals, a normalization procedure was applied with respect to a baseline value acquired from the volunteer blindfolded and acoustically isolated. The physiological parameters vector, defined as $\mathbf{PHY} = [HR, RR, GSR]$, is normalized by removing the patients baseline physiological condition as

$$\mathbf{PHY_r}(t) = \frac{\mathbf{PHY}(t) - \mathbf{PHY_{RB}}}{\mathbf{PHY_{RB}}} \tag{7}$$

where t is the time stamp, $\mathbf{PHY}(t)$ is the physiological vector sampled at the t-th time instant and $\mathbf{PHY_{RB}}$ is the mean physiological parameter vector computed during the resting baseline phase. The physiological responses $\mathbf{PHY_r}$ can be used as input signals to a Fuzzy Logic estimation model to compute the psychophysiological state of the patients in terms of **A** and **V**. For each input signal of $\mathbf{PHY_r}$, three membership functions are generated by using the data collected from all the enrolled participants. In particular, the physiological responses are equally divided into three sets defining the linguistic variables "Low", "Mid", and "High". All the membership functions are built as Gaussian functions fitting the collected data. The **A** and **V** outputs of the Fuzzy Logic

are represented by five equally spaced Gaussian membership functions ranging $\in [0, 1]$. By dividing each dimension into five Gaussians, a categorization of a wide range of human emotional experiences is achieved. This division enables a more precise representation of emotions compared to a simple binary division of positive/negative **V** or low/high **A**. In this way, it is possible to provide insight into the patients' experience in interacting with the rehabilitation robot. The five Gaussians account for "Low", "MidLow", "Mid", "MidHigh", and "High" activations of **A** and **V**. Once the membership functions are defined, conditional fuzzy rules are implemented according to the literature [24].

The psychophysiological adaptation factor δ_{PHY} is computed by the second Fuzzy Logic layer. It aims at continuously mapping the estimated psychophysiological state of the patients in the output variable $\delta_{PHY} \in [0, 2]$, covered by three Gaussian membership functions. The input space, i.e. the psychophysiological state expressed in terms of **A** and **V**, is then represented in the form of "Low1" or "High" activation by means of two Gaussian functions, see the Psychophysiological Adaptation box in Fig. 3. The rules proposed to map the patients' **A** and **V** activations into δ_{PHY} rely on assumptions that aim at modifying the patients' state during the interaction with the robotic device. The assumptions underlying the use of softer or more rigid robot interactions are based on the idea that different emotional states require different types of interaction to optimize the patients' experience and outcomes [30], [31], [32]. Specifically, the rules implemented in the inference system are defined as follows:

- High **A** & High **V**: high involvement with a positive meaning is experimented by the patients. He/she is excited and curious about the interaction with the robot. The robot stiffness only considers the patients motor performance $\delta_{PHY} \rightarrow 1$.
- Low **A** & High **V**: lower Arousal values are associated with a more calm user state. This relaxed condition of the user is not reflected in any modification of the robot behavior $\delta_{PHY} \rightarrow 1$.
- Low **A** & Low **V**: at the beginning of the robot-aided rehabilitation session, the patients may experience feelings of boredom, frustration, and/or absent-mindedness that may preclude the completion of therapy. However, it's important to remember that completing the full rehabilitation session is crucial for the patients' progress and recovery. The rehabilitation robot can intervene more to guarantee the trajectory tracking and stimulate the patients to focus on the task $\delta_{PHY} \rightarrow 2$.
- High **A** & Low **V**: when the patients status is estimated stressed or agitated at the beginning of the session, it is important to adapt the interaction that occurs during the session. A softer and more gentle interaction may help the patients to feel more comfortable and secure. In order to implement such behavior the psychophysiological adaptation factor is $\delta_{PHY} \rightarrow 0$.

Both the Fuzzy Logic models are defined in the MATLAB R2020b exploiting the Fuzzy Logic Toolbox. The Mamdani method is selected to implement the Fuzzy Logic model and the logical AND and OR operators are replaced with $min(\cdot)$ and $max(\cdot)$ respectively. The implication and aggregation methods are $min(\cdot)$ and $max(\cdot)$ respectively. The implemented defuzzification process is the area centroid or center of gravity [24].

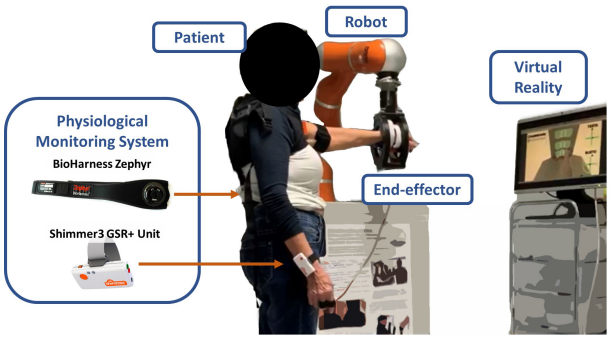

Fig. 4. Experimental setup used to test the proposed approach.

D. Experimental Setup

To validate the proposed pshycophysiological-aware control strategy for robot-aided rehabilitation, the experimental validation is composed of: I) the KUKA LightWeight Robot 4+; II) a purposely designed ergonomic flange to house the patients wrist mounted on the robot end-effector; III) a virtual reality game showing the trajectory to be performed and the actual position; IV) a wearable physiological monitoring system. The robot is controlled through Robot Operating System (ROS) Kinetic middleware on Ubuntu 16.04 LTS. The physiological monitoring system measures the heart and respiration activities and the GSR of the patients. Both the electrical and respiratory activities of the enrolled participants are monitored by using the BioHarness 3.0 chest belt, developed by Zephyr^{TM} Technology. Such a wearable device fuses capacitive and stretch sensors: the former assesses the heart electrical activity, the latter measures the deformations of the rib cage induced by respiration. In order to better measure the electrical changes due to the heart beats, the BioHarness sensor is worn against the skin, at the height of the sternum. The GSR is measured by using two electrodes of the Shimmer 3 GSR+ Unit placed on the index and middle fingers of the non-dominant hand. The physiological data are acquired synchronously under Yet Another Robot Platform (YARP) [33] at 40 Hz.

E. Experimental Protocol

The proposed control strategy was validated in a real clinical setting providing robot-aided rehabilitation on orthopedic patients. Eight patients who suffered from MSDs were enrolled in this study whose characteristics are briefly reported in Table I. In particular, all the enrolled volunteers underwent orthopedic surgical procedures (6 sutures of the rotator cuff and 2 open humerus fractures).

The main objectives of the experimental validation are to assess the robotic platform capabilities in i) adapting the rehabilitation workspace to follow patients' motor recovery in terms of RoM, ii) providing assistance to guide the patients' arm in executing the assigned task by ensuring both spatial and

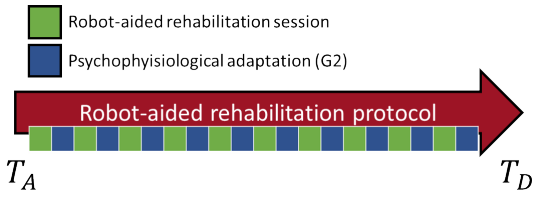

Fig. 5. Experimental protocol to test the psychophysiological-aware control strategy on orthopedic patients.

temporal autonomy and iii) improving the patients' experience in interacting with the rehabilitation robot by taking into account his/her psychophysiological state. In particular, to test this aspect, the enrolled participants were divided into two groups (see Table I): the first one (G1) was provided with the robot-aided treatment with $k_r = k_K$, i. e. $\delta_{PHY} = 1$, the second one (G2) interacted with the robot adjusted with the psychophysiological factor $\delta_{PHY} \in [0, 2]$.

The experimental protocol is composed of twenty daily robot-aided rehabilitation sessions spread over one month, as reported in Fig. 5. During each session, the patients are asked to perform nine cycles of nine 3D point-to-point trajectories, from a starting position toward nine different targets spread on three different heights [34].

In order to assess the motor performance of the patients, two *Kinematics Evaluation sessions* are carried out, i.e. at the admission T_A and at the discharge T_D of each patient. In these sessions, a rest position and nine reachable targets are recorded per patient to obtain a workspace adaptable according to the user RoM. In addition, the participant is asked to complete one cycle of nine point-to-point movements without the robot assistance in order to compute the kinematics performance, in terms of α (see Section II-C.1), and accordingly, tune the stiffness k_K to be provided during the treatment.

Moreover, in ten sessions, i.e. the ones colored in blue in Fig. 5, the patient is equipped with the physiological monitoring system, and his/her psychophysiological state is assessed. The participants belonging to group G2 received the treatment with the robot stiffness accordingly adapted. At the beginning of these experimental rehabilitation sessions, a 5 min *Resting Baseline* is recorded: the patients are asked to sit comfortably, blindfolded, and acoustically isolated to ease their rest condition. The mean values of the physiological parameters collected during the baseline (i.e. P_{RB}) are used in Eq. (7) to compute the physiological responses P_r. At the end of the *Resting Baseline* recording, a further registration lasting 5 minutes takes place. In this acquisition, the patients' psychophysiological state, in terms of initial $\mathbf{A}$ and $\mathbf{V}$, namely A_0 and V_0, is computed and the δ_{PHY} coefficient is determined by following the procedure described in Section II-C.2. At the end of the rehabilitation session, the patients' final psychophysiological state is computed, A_f and V_f, from a 5 minutes physiological data recording.

During all the rehabilitation sessions, the control parameters are set as follows: $k_w = 1000$ N/m, $T_P = 2.5$ s and $T_F = 10.0$ s.

The study was conducted under Ethical Committee approval (Ethical Approval N. 03/19 PAR ComEt CBM) and in accordance with the Declaration of Helsinki. All patients have been adequately informed about the purpose of the study and gave their written informed consent.

TABLE I
CHARACTERISTICS OF THE ENROLLED PATIENTS

Group	ID	Sex	Age	Lesion	Affected Limb
G1	P1	Female	45	Rotator Cuff Lesion	Left
	P2	Female	76	Humerus fracture	Left
	P3	Male	56	Rotator Cuff Lesion	Left
	P4	Female	63	Rotator Cuff Lesion	Right
G2	P5	Female	69	Rotator Cuff Lesion	Right
	P6	Female	79	Humerus fracture	Left
	P7	Male	61	Rotator Cuff Lesion	Left
	P8	Male	48	Rotator Cuff Lesion	Left

F. Performance Indicators

In order to assess the robotic system capabilities in assisting the patients and letting they free to move with a certain degree of both spatial and temporal autonomy, some performance indicators are computed during the rehabilitation session subsequent to each *Evaluation sessions* (in order to record information with the k_K updated).

1) Position Error (PE): the mean value of the norm along with the standard deviation of the errors computed in all the time stamp t of a performed movement, namely $\|\tilde{p}(t)\| = \|p_T(t) - p_a(t)\|$, represents the PE. It is the controller error in tracking the planned path and quantitatively measures the patients spatial autonomy.
2) Rehabilitation Workspace Volume (RWV): the volume of the convex hull (expressed in m^3) of the patients' reachable workspace is computed. Given all the Cartesian positions recorded by the patients during the evaluation session, the volume of the three-dimensional convex hull can be computed by means of the quick hull algorithm presented in [35]. This performance indicator aims at demonstrating that the robot is capable of managing various volumes according to the patients' RoM.
3) Task Completion Time (TCT): the mean time, and the standard deviation, required for the patients to perform the assigned task are computed. In particular, the TCT allows verifying that the patients benefit from a certain degree of temporal autonomy.
4) Motion Speed (MS): another performance indicator used to assess the user's temporal autonomy is the MS. It is computed as the mean value and standard deviation of the patients' motion velocity during a rehabilitation session.
5) Total Interaction Force (TIF): it is the mean value, along with the standard deviation, of the norm of the total interaction force that the robot exchanges with the environment, i. e. the patients, per each performed movement.

The sessions subsequent to each *Kinematics Evaluation sessions* are selected to compute the aforementioned performance

indicators. In these sessions, the robot stiffness is $k_r = k_K$ (i.e. $\delta_{PHY} = 1$) for all the enrolled patients.

Furthermore, the psychophysiological state modification is computed in the ten experimental treatments. It is computed in terms of $\Delta A = (A_f - A_0)$ and $\Delta V = (V_f - V_0)$. The psychophysiological-aware controller implemented aims at increasing the valence of the interaction ($\Delta V > 0$).

Lastly, in order to quantify the efficacy of the robot-aided treatment, the aforementioned aiming-angle α and the Constant-Murley Score (CMS) were used [36]. The former is a kinematic performance indicator objectively measured by the robotic system, the latter is a clinical score ranging from 0 to 100 assessing the shoulder quality of the motor functions.

G. Statistical Analysis

In order to evaluate the impact of the psychophysiological-aware control strategy with respect to the conventional robotic treatment, i.e. computed on the two experimental patient groups G1 and G2, a statistical analysis has been carried out on the aforementioned performance indicators. The Wilcoxon rank-sum test is performed on the computed metrics. This test assesses whether a significant difference exists between the investigated conditions. In particular, the significance level was set for p-value ≤ 0.05. Moreover, for each group of participants, the performance at admission and discharge was compared using the same statistical analysis. In order to assess the psychophysiological state modification over the treatment, ΔA and ΔV were averaged across the ten experimental sessions per patient.

III. Results and Discussions

Fig. 6 shows insight into the desired trajectories and the performed ones executed by a healthy participant (HP) obtained at $k_r = \{1000, 300\}$ N/m and a representative patient (P5) during two rehabilitation sessions, i. e. the admission (T_A) and the discharge (T_D). It is evident how the proposed control strategy allows healthy and orthopedic participants to track a Cartesian reference trajectory. As the radial stiffness of the implemented control decreases, it is observed that the subject can deviate from the assigned trajectory with greater freedom. Analysing the reported patients behaviour in more detail, at the beginning of the treatment, the kinematics performance of the patients is reduced ($\alpha = 0.49 \pm 0.19$), so the kinematics stiffness is accordingly set at its maximum value ($k_K = 1000$ N/m). As evident, the point-to-point movements, reported in Fig. 6A, are performed with high accuracy. In other words, the patients' limb is accurately kept near the desired path so he/she experimented a little degree of spatial autonomy. At the end of the rehabilitation protocol, the patients' motor performance improves ($\alpha = 0.26 \pm 0.08$) so the controller parameters are accordingly tuned. The kinematics stiffness is set at $k_K = 300$ N/m letting the patients free to move with a higher degree of spatial autonomy. As emerges from Fig. 6B, the robot controller admits the patient making higher position errors during the execution of the assigned tasks. Moreover, it is worth observing that at the end of the treatment, the RWV is greater. The patient recovers its RoM so she can reach a wider space region.

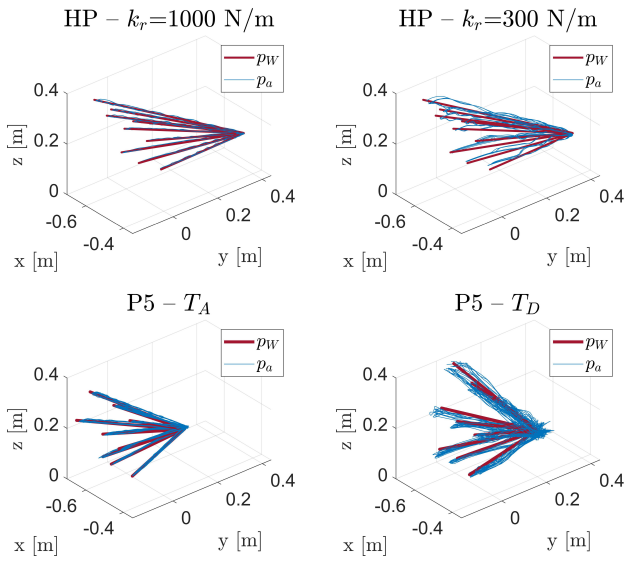

Fig. 6. Trajectories executed by a healthy participant (HP) at different radial stiffnesses k_r are reported in the first row. The second row reports the trajectories of P5 at the admission and discharge (T_A and T_D), respectively. The desired and actual trajectories are colored in red and blue in all the plots.

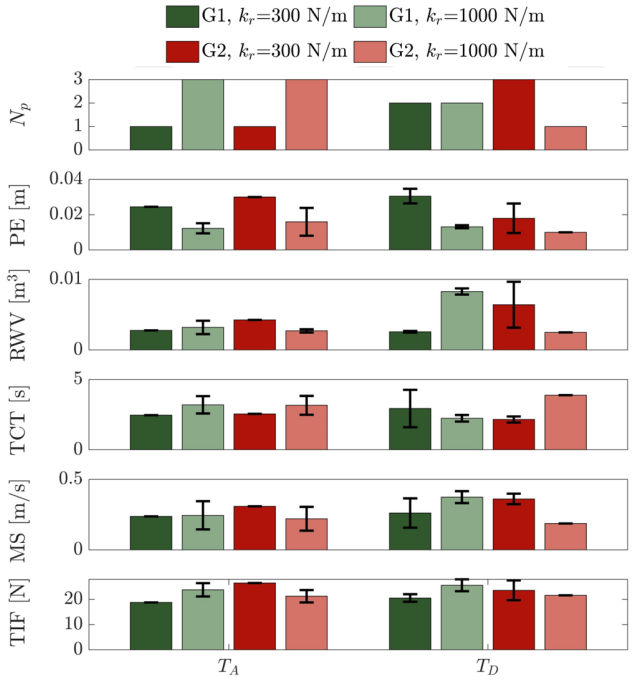

Fig. 7. Performance indicators computed for the enrolled patients. Results are stratified for the two groups of patients and stiffnesses k_r.

Table II reports the performance indicators introduced in Section II-F, averaged over the two groups of participants.

Since the robot stiffness plays an essential role in determining the performance indicators, the results were also stratified on the basis of radial stiffness k_r. Fig. 7 presents the results aggregated by group and robot stiffness k_r. In particular, the first row reports the number of patients N_p per each group.

TABLE II
AGGREGATED PERFORMANCE INDICATORS COMPUTED FOR THE TWO PATIENTS GROUPS

	T_A		T_D	
	G1	G2	G1	G2
PE [m]	0.015 ± 0.006	0.014 ± 0.004	0.021 ± 0.010	0.027 ± 0.013
RWV [m^3]	0.003 ± 0.001	0.002 ± 0.001	0.005 ± 0.003	0.004 ± 0.002
TCT [s]	3.01 ± 0.62	1.99 ± 0.45	2.59 ± 0.87	1.55 ± 0.58
MS [m/s]	0.24 ± 0.08	0.42 ± 0.06	0.32 ± 0.09	0.57 ± 0.24
TIF [N]	22.5 ± 3.3	19.2 ± 5.5	23.0 ± 3.3	19.5 ± 4.2

The higher the radial stiffness k_r implemented in the controller, the lower the PE. That means the patients experiment with higher degrees of spatial autonomy when the radial stiffness decreases. The patients are more and more able to freely move in a space region around the planned path P as his/her kinematics performance improves.

Another essential feature of the implemented system is its capability to adapt the rehabilitation workspace according to the reachable volume of the specific patient, i. e. according to his/her RoM. The RWV performance indicator highlights that the volume spanned by the robot in different rehabilitation sessions varies per each specific user and session. Furthermore, it is worth observing that the RWV mostly increments for the enrolled participant over time: the patients are capable of spanning a wider space region at the discharge. In particular, the computed values are $RWV = 0.002 \pm 0.001$ m^3 and $RWV = 0.005 \pm 0.003$ m^3 at T_A and T_D, respectively. The aggregated results presented in Table II highlighs that the G1 patients were able to cover a significantly larger volume at T_A with respect to G2 participants ($p_{value} = 0.04$). At the discharge, such differences were no longer significant.

The temporal autonomy of the patients in executing the proposed motor tasks is objectively quantified by means of TCT and MS indicators. All the enrolled participants take less time than the implemented maximum time $T_F = 10.0$ s and in general, they anticipate the implemented back-wall (that starts after $T_P = 2.5$ s) so that the assistive back-wall contributions are exerted by the controller only when the patients are slacking or moving too slow. As evident from Fig. 7, all the participants in all the analyzed sessions can move at their own motion speed to accomplish the task, meaning they all benefit from high temporal autonomy. Such an aspect overcomes the drawbacks of the previously mentioned approaches based on velocity fields [12]. Moreover, it can be noticed from Table II that G2 patients could move faster, i.e. with a greater MS and a lower TC, in both T_A and T_D sessions. However, these differences were not statistically significant (TC in T_D computed between G1 and G2 returned $p_{value} = 0.07$).

The TIF is computed to quantify the interaction forces exerted by the robot during the rehabilitation treatments. It is worth observing that the mean force does not significantly change between the two analyzed sessions per patient. What can be emphasized from Table II is that patients in the G2 group require fewer assistive interventions compared to patients in the G1 group.

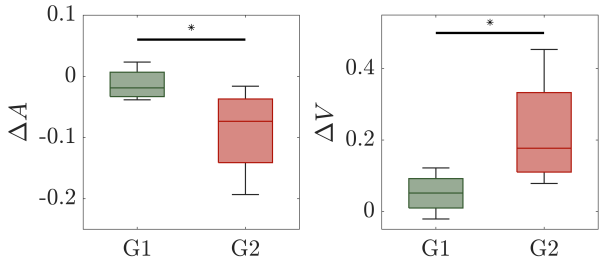

Fig. 8. Psychophysiological state modification computed for the enrolled participants averaged over the ten experimental sessions. In particular, the G2 patients undergo rehabilitation treatments with a stiffness adapted according to the estimated psychophysiological condition. The black stars represent statistically significant differences between the two groups.

Fig 8 reports the psychophysiological state modification computed for the enrolled participants averaged across the ten experimental sessions. In particular, the results are divided into the two subgroups of participants (G1 and G2). It is worth observing that both groups exhibit similar psychophysiological behaviours: **A** decreases and **V** increases after the robot-aided rehabilitation session. On the other hand, it is evident that the G2 patients, the ones receiving the δ_{PHY} stiffness adaptation, have a higher psychophysiological state modification. In particular, ΔA are -0.01 ± 0.02 and -0.08 ± 0.07 (Wilcokson rank sum test returned a $p_{value} = 0.04$) and ΔV are 0.05 ± 0.05 and 0.22 ± 0.16 ($p_{value} = 0.03$) for groups G1 and G2, respectively. These results evidence that taking into account the psychophysiological state of the patients in the robot control parameters has an impact on the patients themself. The considerations drawn to design the δ_{PHY} coefficient can adjust the robot stiffness to drive the patients in a calm condition.

Fig. 9 shows the clinical outcomes of the enrolled patients in terms of α and CMS. The aiming angles reported in the figure are those obtained by the patients performing nine point-to-point movements in their reachable workspace with the robot set in transparent mode, i.e. k_w and k_r set at 0. As evident, both groups improved significantly their accuracy in performing a straight movement after twenty sessions of upper limb robot-aided rehabilitation. In particular, the rank-sum test returned p-values of 0.008 and < 0.001 for G1 and G2, respectively. Moreover, it is worth observing that participants of G2 obtained a significantly better kinematic performance with respect to G1 at the discharge (p-value$=$ 0.008). These results mean that the patients who interacted with the psychophysiological-aware controller exhibited a

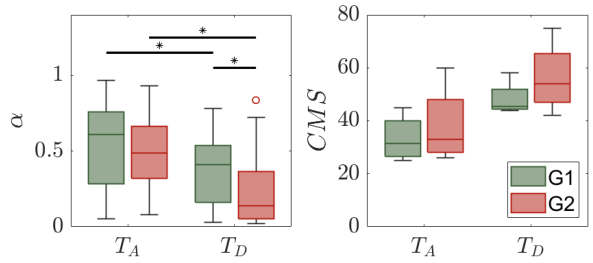

Fig. 9. Clinical outcomes of the enrolled patients. The α is assessed by means of the robot and the CMS is a clinical score administered by a physiotherapist. The black stars represent statistically significant differences between the two groups.

greater kinematic improvement over time. From a clinical point of view, the shoulder function, assessed with the CMS, improved for both groups of enrolled patients. In particular, the p-values computed for G1 and G2 when comparing T_A and T_D are 0.2 and 0.08, respectively. Moreover, it is evident that the patients of the G2 group reported greater functionality of the shoulder compared to the G1 group. Nevertheless, the differences highlighted among the groups and the evaluation session resulted to be not statistically significant (p-value$=$ 0.68).

To summarize, the psychophysiological-aware control strategy has been shown to be effective in delivering a specific treatment tailored to a single patient. The controller itself proved to be capable of delivering assistive contributions to let the patients interact with the robot to accomplish motor tasks at their specific speed. Moreover, the assistance tuned according to the user's kinematic and psychophysiological status allows engaging the participants of the experimental group (G2) in all the rehabilitation sessions. Indeed, their psychophysiological status moved to calmer and more relaxed states from the beginning of the therapy with respect to the one those who interacted with the robot characterized by the same stiffness value in all the sessions. The psychophysiological assessment also makes it possible to assess when to stop treatment in a given session. As stressed above, orthopedic patients do not need intensive treatment like neurological ones but need to train the affected joints in progressive elongation and recovery of muscle strength without generating excessive fatigue and/or frustration.

The proposed patient tailoring approach had an impact also on the motor performance of the participants. The G2 better improved their kinematic performance, quantified in terms of α. Anyhow, the clinical outcome, assessed with the CMS, revealed that all the enrolled patients exhibited an improvement in their shoulder quality of motor function even if these modifications are not statistically significant.

Although the results shown in this work are of great impact in terms of pushing research in the direction of precision medicine, the obtained experimental results should be considered preliminary due to the small sample size and heterogeneity of the enrolled population. It is shown that the tailoring of the robotic rehabilitation treatment has an evident effect on the motor performance of the patients, but further analysis to clinically validate the system with respect to a control group is needed.

IV. Conclusion

This paper proposed a psychophysiological-aware control strategy for upper-limb orthopedic rehabilitation. The main features of the implemented robotic systems are the capability of generating point-to-point trajectories inside an adaptable rehabilitation workspace, providing assistance as needed to allow the patients to experiment with certain degrees of spatial and temporal autonomy, and tuning the assistance level according to patients' kinematics performance as well as his/her psychophysiological state. In particular, the control law takes into account the psychophysiological state of the patients in order to provide a highly tailored treatment having an impact on their human-robot interaction experience. The implemented robotic platform is validated in a real clinical setting by enrolling eight orthopedic patients who undergo twenty robot-aided rehabilitation sessions. The claimed capabilities of the control strategy are quantified in this experimental setting. The main findings of the present study are that patients who interacted with the robot tailored to their psycho-physiological state lead patients into calmer and more relaxed states than when they are starting the rehabilitation session. Moreover, the effects of robotic treatment are reflected in the results obtained by calculating specific performance indicators of motor recovery. Patients become able to perform straight movements accurately after twenty sessions of robotic rehabilitation.

The proposed psychophysiological-aware control strategy for upper-limb orthopedic rehabilitation is a step forward in robot-aided rehabilitation as it proved that tailoring the treatment according to the specific patient needs improves the outcome of the rehabilitation process. Future work will be devoted to clinically validating the proposed approach by comparing the clinical outcomes with respect to a control group performing conventional therapy.

References

[1] (2014). *Tiring or Painful Positions*. [Online]. Available: https://osha.europa.eu/en/surveys-and-statistics-osh/esener/2014

[2] A. E. Dembe, J. B. Erickson, and R. Delbos, "Predictors of work-related injuries and illnesses: National survey findings," *J. Occupational Environ. Hygiene*, vol. 1, no. 8, pp. 542–550, Aug. 2004.

[3] P. Hämäläinen, K. L. Saarela, and J. Takala, "Global trend according to estimated number of occupational accidents and fatal work-related diseases at region and country level," *J. Saf. Res.*, vol. 40, no. 2, pp. 125–139, 2009.

[4] A. Williams et al., "Musculoskeletal conditions may increase the risk of chronic disease: A systematic review and meta-analysis of cohort studies," *BMC Med.*, vol. 16, no. 1, pp. 1–9, Dec. 2018.

[5] C. Nerz, L. Schwickert, C. Becker, S. Studier-Fischer, J. A. Müßig, and P. Augat, "Effectiveness of robot-assisted training added to conventional rehabilitation in patients with humeral fracture early after surgical treatment: Protocol of a randomised, controlled, multicentre trial," *Trials*, vol. 18, no. 1, pp. 1–9, Dec. 2017.

[6] M. A. Padilla-Castañeda et al., "An orthopaedic robotic-assisted rehabilitation method of the forearm in virtual reality physiotherapy," *J. Healthcare Eng.*, vol. 2018, pp. 1–20, Aug. 2018.

[7] K. Parmelee-Peters and S. W. Eathorne, "The wrist: Common injuries and management," *Primary Care, Clinics Office Pract.*, vol. 32, no. 1, pp. 35–70, Mar. 2005.

[8] M. K. Dekkers and T. L. Nielsen, "Occupational performance, pain, and global quality of life in women with upper extremity fractures," *Scandin. J. Occupational Therapy*, vol. 18, no. 3, pp. 198–209, Sep. 2011.

[9] M. Mihelj, D. Novak, J. Ziherl, A. Olenšek, and M. Munih, "Challenges in biocooperative rehabilitation robotics," in *Proc. IEEE Int. Conf. Rehabil. Robot.*, 2011, pp. 1–6.

[10] H. I. Krebs et al., "Rehabilitation robotics: Performance-based progressive robot-assisted therapy," *Autonom. Robot.*, vol. 15, no. 1, pp. 7–20, Jul. 2003.

[11] L. Zhang, S. Guo, and Q. Sun, "An assist-as-needed controller for passive, assistant, active, and resistive robot-aided rehabilitation training of the upper extremity," *Appl. Sci.*, vol. 11, no. 1, p. 340, Dec. 2020.

[12] H. J. Asl, M. Yamashita, T. Narikiyo, and M. Kawanishi, "Field-based assist-as-needed control schemes for rehabilitation robots," *IEEE/ASME Trans. Mechatronics*, vol. 25, no. 4, pp. 2100–2111, Aug. 2020.

[13] C. Tamantini et al., "Patient-tailored adaptive control for robot-aided orthopaedic rehabilitation," in *Proc. Int. Conf. Robot. Autom. (ICRA)*, May 2022, pp. 5434–5440.

[14] C. Camardella et al., "A random tree forest decision support system to personalize upper extremity robot-assisted rehabilitation in stroke: A pilot study," in *Proc. Int. Conf. Rehabil. Robot. (ICORR)*, Jul. 2022, pp. 1–6.

[15] R. S. Calabró et al., "Toward improving functional recovery in spinal cord injury using robotics: A pilot study focusing on ankle rehabilitation," *Exp. Rev. Med. Devices*, vol. 19, no. 1, pp. 83–95, Jan. 2022.

[16] R. Riener and M. Munih, "Guest editorial special section on rehabilitation via bio-cooperative control," *IEEE Trans. Neural Syst. Rehabil. Eng.*, vol. 18, no. 4, pp. 337–338, Aug. 2010.

[17] F. S. di Luzio et al., "Bio-cooperative approach for the human-in-the-loop control of an end-effector rehabilitation robot," *Frontiers Neurorobotics*, vol. 12, p. 67, Oct. 2018.

[18] A. Koenig, X. Omlin, D. Novak, and R. Riener, "A review on bio-cooperative control in gait rehabilitation," in *Proc. IEEE Int. Conf. Rehabil. Robot.*, Jun. 2011, pp. 1–6.

[19] A. Koenig wt al., "Psychological state estimation from physiological recordings during robot-assisted gait rehabilitation," *J. Rehabil. Res. Develop.*, vol. 48, no. 4, pp. 367–385, 2011.

[20] C. R. Guerrero, J. F. Marinero, J. P. Turiel, and P. R. Farina, "Bio cooperative robotic platform for motor function recovery of the upper limb after stroke," in *Proc. Annu. Int. Conf. IEEE Eng. Med. Biol.*, Aug. 2010, pp. 4472–4475.

[21] I. Pecoraro et al., "Psychophysiological assessment of exoskeleton-assisted treadmill walking," in *Proc. Int. Conf. NeuroRehabilitation*. Cham, Switzerland: Springer, 2020, pp. 201–205.

[22] K. Stanisławski, J. Cieciuch, and W. Strus, "Ellipse rather than a circumplex: A systematic test of various circumplexes of emotions," *Personality Individual Differences*, vol. 181, Oct. 2021, Art. no. 111052.

[23] D. Novak, M. Mihelj, J. Ziherl, A. Olensek, and M. Munih, "Psychophysiological measurements in a biocooperative feedback loop for upper extremity rehabilitation," *IEEE Trans. Neural Syst. Rehabil. Eng.*, vol. 19, no. 4, pp. 400–410, Aug. 2011.

[24] F. J. Badesa et al., "Dynamic adaptive system for robot-assisted motion rehabilitation," *IEEE Syst. J.*, vol. 10, no. 3, pp. 984–991, Sep. 2016.

[25] B. F. Villar, P. F. Viñas, J. P. Turiel, J. C. F. Marinero, and A. Gordaliza, "Influence on the user's emotional state of the graphic complexity level in virtual therapies based on a robot-assisted neuro-rehabilitation platform," *Comput. Methods Programs Biomed.*, vol. 190, Jul. 2020, Art. no. 105359.

[26] F. Özkul, D. E. Barkana, and E. Masazade, "Dynamic difficulty level adjustment based on score and physiological signal feedback in the robot-assisted rehabilitation system, RehabRoby," *IEEE Robot. Autom. Lett.*, vol. 6, no. 2, pp. 447–454, Apr. 2021.

[27] C. Tamantini, C. Lauretti, F. Cordella, and L. Zollo, "A dataset of DMPS for robot motion planning," in *Proc. Conf. Paper*, 2020, pp. 202–205.

[28] C. Lauretti, F. Cordella, C. Tamantini, C. Gentile, F. S. D. Luzio, and L. Zollo, "A surgeon-robot shared control for ergonomic pedicle screw fixation," *IEEE Robot. Autom. Lett.*, vol. 5, no. 2, pp. 2554–2561, Apr. 2020.

[29] L. Zhang, S. Guo, and Q. Sun, "Development and assist-as-needed control of an end-effector upper limb rehabilitation robot," *Appl. Sci.*, vol. 10, no. 19, p. 6684, Sep. 2020.

[30] C. Bartneck, D. Kulić, E. Croft, and S. Zoghbi, "Measurement instruments for the anthropomorphism, animacy, likeability, perceived intelligence, and perceived safety of robots," *Int. J. Social Robot.*, vol. 1, no. 1, pp. 71–81, Jan. 2009.

[31] A. Ajoudani, A. M. Zanchettin, S. Ivaldi, A. Albu-Schäffer, K. Kosuge, and O. Khatib, "Progress and prospects of the human–robot collaboration," *Auto. Robots*, vol. 42, no. 5, pp. 957–975, Jun. 2018.

[32] P. K. John, X. Zhu, T. Gedeon, and W. Zhu, "Evaluating human impressions of an initiative-taking robot," in *Proc. CHI Conf. Human Factors Comput. Syst. Extended Abstr.*, Apr. 2022, pp. 1–7.

[33] G. Metta, P. Fitzpatrick, and L. Natale, "YARP: Yet another robot platform," *Int. J. Adv. Robotic Syst.*, vol. 3, no. 1, p. 8, Mar. 2006.

[34] C. Tamantini, F. Cordella, C. Lauretti, and L. Zollo, "The WGD—A dataset of assembly line working gestures for ergonomic analysis and work-related injuries prevention," *Sensors*, vol. 21, no. 22, p. 7600, Nov. 2021.

[35] C. B. Barber, D. P. Dobkin, and H. Huhdanpaa, "The quickhull algorithm for convex hulls," *ACM Trans. Math. Softw.*, vol. 22, no. 4, pp. 469–483, Dec. 1996.

[36] V. B. Conboy, R. W. Morris, J. Kiss, and A. J. Carr, "An evaluation of the constant-murley shoulder assessment," *J. Bone Joint Surgery. Brit. Volume*, vol. 78, no. 2, pp. 229–232, Mar. 1996.

Open Access funding provided by 'Università "Campus Bio-Medico" di Roma' within the CRUI CARE Agreement